NASA/TM—2003-212473

The Effect of Heat Treatment on the Fatigue Behavior of Alloy 10

John Gayda
Glenn Research Center, Cleveland, Ohio

Pete Kantzos
Ohio Aerospace Institute, Brook Park, Ohio

Jack Telesman
Glenn Research Center, Cleveland, Ohio

August 2003

The NASA STI Program Office . . . in Profile

Since its founding, NASA has been dedicated to the advancement of aeronautics and space science. The NASA Scientific and Technical Information (STI) Program Office plays a key part in helping NASA maintain this important role.

The NASA STI Program Office is operated by Langley Research Center, the Lead Center for NASA's scientific and technical information. The NASA STI Program Office provides access to the NASA STI Database, the largest collection of aeronautical and space science STI in the world. The Program Office is also NASA's institutional mechanism for disseminating the results of its research and development activities. These results are published by NASA in the NASA STI Report Series, which includes the following report types:

- TECHNICAL PUBLICATION. Reports of completed research or a major significant phase of research that present the results of NASA programs and include extensive data or theoretical analysis. Includes compilations of significant scientific and technical data and information deemed to be of continuing reference value. NASA's counterpart of peer-reviewed formal professional papers but has less stringent limitations on manuscript length and extent of graphic presentations.

- TECHNICAL MEMORANDUM. Scientific and technical findings that are preliminary or of specialized interest, e.g., quick release reports, working papers, and bibliographies that contain minimal annotation. Does not contain extensive analysis.

- CONTRACTOR REPORT. Scientific and technical findings by NASA-sponsored contractors and grantees.

- CONFERENCE PUBLICATION. Collected papers from scientific and technical conferences, symposia, seminars, or other meetings sponsored or cosponsored by NASA.

- SPECIAL PUBLICATION. Scientific, technical, or historical information from NASA programs, projects, and missions, often concerned with subjects having substantial public interest.

- TECHNICAL TRANSLATION. English-language translations of foreign scientific and technical material pertinent to NASA's mission.

Specialized services that complement the STI Program Office's diverse offerings include creating custom thesauri, building customized databases, organizing and publishing research results . . . even providing videos.

For more information about the NASA STI Program Office, see the following:

- Access the NASA STI Program Home Page at ***http://www.sti.nasa.gov***

- E-mail your question via the Internet to help@sti.nasa.gov

- Fax your question to the NASA Access Help Desk at 301–621–0134

- Telephone the NASA Access Help Desk at 301–621–0390

- Write to:
  NASA Access Help Desk
  NASA Center for AeroSpace Information
  7121 Standard Drive
  Hanover, MD 21076

NASA/TM—2003-212473

The Effect of Heat Treatment on the Fatigue Behavior of Alloy 10

John Gayda
Glenn Research Center, Cleveland, Ohio

Pete Kantzos
Ohio Aerospace Institute, Brook Park, Ohio

Jack Telesman
Glenn Research Center, Cleveland, Ohio

National Aeronautics and
Space Administration

Glenn Research Center

August 2003

Document History

This research was originally published internally as AST032 in February 2000.

The Propulsion and Power Program at
NASA Glenn Research Center sponsored this work.

Available from

NASA Center for Aerospace Information
7121 Standard Drive
Hanover, MD 21076

National Technical Information Service
5285 Port Royal Road
Springfield, VA 22100

Available electronically at http://gltrs.grc.nasa.gov

INTRODUCTION

Gas turbine engines for future subsonic aircraft will probably have higher pressure ratios which require nickel-base superalloy disks with 1300 to 1400°F temperature capability. Several advanced disk alloys are being developed to fill this need. Under NASA's AST Program, manufacturing technologies for two advanced disk alloys, were studied by a team representing four engine companies, GEAE, PWA, Allied Signal, and Allison. GEAE and PWA focused their attention on an advanced disk alloy suitable for large engine applications developed under NASA's HSR Program, while Allied Signal and Allison opted to focus their attention on Alloy 10, a high strength nickel-base disk alloy, which was developed by Allied Signal for application in smaller gas turbine engines. Eight heat treat options for Alloy 10 were studied by Allison and Allied Signal. The production, heat treatment, and initial evaluation, i.e. tensile and creep properties, of eight forgings of Alloy 10 were run under the AST Disk Program. However, due to funding limitations, fatigue and crack growth evaluation of the eight forgings were moved to NASA's Ultrasafe Project. These properties are critical for safe operation of compressor and turbine disks.

The results of the fatigue evaluation on Alloy 10, run under NASA's Ultrasafe Project, are the subject of this report. Crack growth evaluation will be examined in a separate report. The eight heat treatments studied were designed to evaluate the effect of solution temperature, cooling rate, and stabilization on key mechanical properties of Alloy 10, including fatigue life. Two temperatures were studied, 750 and 1300°F, which represent projected application temperatures for the bore and rim locations in a disk. In addition to fatigue life, the cyclic stress-strain response and failure modes of the fatigue specimens are also reviewed in this report.

MATERIAL AND PROCEDURES

Alloy 10 is a high strength nickel-base superalloy, with a gamma prime content of about 55%. Its composition is shown in Table I. Due to the alloy's high gamma prime content it is generally produced using a powder metallurgy technique. For this study, argon atomized powder was produced from remelt stock by Special Metals Corporation, which was subsequently screened to –270 mesh, canned, and hot isostatically pressed (HIP) at 2000°F and 15KSI for 3 hours. The HIP billet was then extruded at 2025°F using a 6:1 extrusion ratio. After ultrasonic inspection, forging mults were cut from the extrusion and isothermally forged into "pancake" shapes about 14" in diameter and 2" thick by Wyman-Gordon. More details on the exact processing history can be found in Reference 1.

Eight forgings were given different heat treatments, defined in Table II. As previously stated, these heat treat options were designed to study the effect of solution temperature, cooling rate, and stabilization. Solution temperatures were selected based on the gamma prime solvus, about 2160°F for Alloy 10, and were used to set alloy grain size. Three solution temperatures were employed, 2125, 2160, and 2190°F. These solution temperatures were intended to produce target grain sizes of ASTM 11, 8, and 5

respectively. The cooling rate from the solution temperature is known to impact mechanical properties and was therefore varied as follows. Fan cooling, which gives moderately fast cooling rates, was applied at all three solution temperatures. Faster cooling rates were also tried at 2125°F (oil quench) and 2160°F (1200°F salt bath quench) solution temperatures. A slow, controlled cooling scheme, in which a forging is cooled at an initial rate of 3°F per minute to 2160°F and then fan cooled, was also tried at the 2190°F solution temperature. This cooling scheme is designed to enhance grain boundary serrations which are thought to benefit dwell crack growth properties. The effect of a stabilization treatment, 1550°F for 4 hours, was studied for oil quenched forgings with the 2125°F solution treatment and fan cooled forgings with the 2190°F solution treatment. Stabilization treatments are used to minimize residual stresses, but are also known to impact mechanical properties by coarsening gamma prime precipitates and promoting the formation of $Cr_{23}C_6$ carbides. A final age, 1400°F for 16 hours, was also applied as the last step in all heat treatments. A more detailed description of the heat treatments can be found in Reference 1.

Fatigue tests were run on specimens of the design and orientation shown in Figure 1. As previously stated tests were run at 750 and 1300°F. All heat treat variants of Alloy 10 were evaluated at 750F. At 1300F, only three heat treat variants with differing grain sizes were evaluated, identified as B2, E1, and C2 in Table II. The choice of these three heat treat variants also spans the spectrum of tensile strength in this study. At the onset of testing, a strain-controlled, zero-tension waveform was employed with a frequency of 0.3HZ. Based on disk requirements, target strain ranges of 0.6, 0.7, 0.85, and 1.4% were evaluated. After 24 hours, a 10HZ load-controlled waveform was employed during the remainder of the test using the stabilized loads established under strain control. All tests were run to failure. The fracture surfaces of selected specimens were examined with an SEM to determine failure modes.

RESULTS AND DISCUSSION

Microstructure. The heat treatments studied in this report produced a range of microstructures. As seen in Table III, the choice of solution temperatures resulted in grain sizes near the intended values for all heat treatments except D1. The fine grain size of D1, ASTM 12, indicates that the solution temperature never reached 2160°F and probably was closer to the subsolvus solution temperature, 2125°F. Higher solution temperatures promoted increased porosity levels as well as coarser grain sizes. At the highest solution temperature, 2190°F, porosity levels approached 1% and, as seen in Figure 2, appeared to be associated with grain boundary triple points. This suggests that much of the porosity may have been associated with incipient melting at the highest solution temperature. A small quench crack was also observed in one of the forgings solutioned at 2190°F, C2. However, a majority of the forging was crack free and utilized for mechanical testing. Differences in cooling rates and solution temperatures produced noticeable variations in the size of gamma prime precipitates as seen in Figure 3. As expected oil and salt bath quenching produced significantly finer gamma prime precipitates than fan cooling. Lower solution temperatures also promoted finer gamma prime precipitates.

Monotonic Properties. Before examining the fatigue results, a short review of tensile and creep properties from Reference 1 is warranted. Figures 4 and 5 compare tensile properties for the various heat treatments studied at 800 and 1300°F respectively. As one might expect, yield and tensile strength are significantly lower at 1300°F for all heat treatments. At both test temperatures, lower solution temperatures, which produce finer grain size, promoted higher strength. Faster cooling rates, which produce finer cooling γ', also increase tensile strength at both test temperatures. Unlike other disk alloys, stabilization produced little change in tensile strength. Ductility levels for all heat treatments were similar at 800°F, about 20% for all heat treatments. However, at 1300°F ductility was clearly affected by solution temperature. Subsolvus solution conditions produced a significant decrease in ductility. Time to 0.2% creep, an important design consideration for disks, was also measured at 1300°F/100KSI and is plotted in Figure 6. Unlike tensile strength, creep testing showed higher solution temperatures, i.e. larger grain size, enhanced creep resistance. Further, stabilization was found to have a deleterious impact on creep resistance. This effect was more pronounced for the subsolvus solution cycle although the supersolvus solution cycle also exhibited a substantial loss in creep resistance with stabilization. In summary, the trends observed for tensile and creep properties were, for the most part, anticipated and clearly demonstrate the high strength potential of Alloy 10.

Cyclic Deformation. The cyclic stress-strain response of Alloy 10 was found to be relatively stable for fatigue tests at 750 and 1300°F. Stress range versus strain range data for heat treatments B2, E1, and C2, at cycle one and half life, are plotted in Figure 7. Recall that these three heat treatments span the range of grain size and tensile strength in this study. The difference in stress range, for a given heat treatment and strain range, clearly shows a decrease on going from 750 to 1300°F. However, for a given heat treatment and temperature, little change in stress range is noted between cycle one and half life at all but the largest strain range, 1.4%. At that strain range, there appears to be a small increase at 750 and 1300°F. A parabolic fit to the data in these plots is also shown in Figure 7 and summarized in Table IV. For completeness the 750F parabolic parameters for heat treats B1, C1, D2, D1, and E2 are also included. If one plots the calculated stress range, from Table IV, versus alloy yield strength for a given strain range, the expected trend between the two is readily observed, Figure 8.

Maximum stress versus strain range data for heat treatments B2, E1, and C2, at cycle one and half life, are plotted in Figure 9. As with stress range, maximum stress levels clearly show a decrease on going from 750 to 1300°F for a given heat treatment and strain range. Maximum stress is also seen to increase with alloy yield strength, recall B1, E1, and C2 represent heat treatments which give progressively lower yield strength. However, little change is seen between cycle one and half life, for a given heat treatment and temperature, except at the largest strain range. At that level, the maximum stress tends to increase at 750°F but decrease at 1300°F. This difference is undoubtedly due to the effect of creep at 1300°F. A linear fit to the data in these plots is also shown in Figure 9 and summarized in Table V. Once again the linear coefficients for all heat treatments at 750°F are included in Table V for completeness. A plot of calculated maximum stress

level versus alloy yield strength, shown in Figure 10, also reinforces the trend between these two factors noted in Figure 9.

The stability of the cyclic stress-strain response at all but the largest strain range is in part due to the fact that the inelastic strain at half life was quite small for these tests, less than .02%. At the largest strain range, 1.4%, inelastic strains were much greater as seen in Table VI. As one might expect, the level of inelastic strain tends to increase as alloy yield strength decreases and temperature increases.

Fatigue Life. Test temperature was found to alter fatigue life of Alloy 10. At 750°F the eight heat treatments appear to fall into three groups as suggested by the three curves plotted with the data in Figure 11. The heat treatments with a subsolvus solution had significantly better fatigue lives than the heat treatments with a supersolvus solution. The fatigue life of the near solvus solution heat treatment, E1, is intermediate. Note heat treatment D2 is considered a subsolvus heat treatment based on grain size result, Table III. While the data for the supersolvus heat treatments does show a small but consistent difference between D1 and E2, the heat treatments with a subsolvus solution show little if any differentiation as a result of cooling rate or stabilization. Based on this observation it would appear that grain size differences, not strength differences, is the dominant factor responsible for segregating the data at 750°F. This hypothesis is supported by fractographic examination of failure surfaces that showed a predominance of facet initiations at 750°F which mirror alloy grain size, Figure 12.

At 1300°F, a comparison of heat treatments B2, E1, and C2 suggests that fatigue lives for all three are similar above 0.6%, Figure 13. At 0.6% there is a significant spread in the data for heat treatments B2 and E1, subsolvus and near solvus, but C2, the supersolvus heat treatment, has a low but consistent life around 25,000 cycles. These results indicate that grain size is not as important at 1300°F as it was at 750°F. In fact, fractographic examination of failure surfaces show porosity related initiation is more prevalent at 1300°F, Figure 14, especially for heat treatment C2 which had the highest solution temperature. As previously stated, porosity level increased with solution temperature. These facts suggest that the fatigue life of Alloy 10 is relatively insensitive to microstructural features and strength differences at 1300°F, but porosity appears to be important especially at low strain ranges. This would not only explain the low life for the supersolvus heat treatment, C2, at 0.6%, but also accounts, at least to some degree, for the scatter in heat treatments E1 and B2, as the severity and frequency of pore formation decreases with decreasing solution temperature. The parabolic curve fit in Figure 13 is based on the pooled data for heat treatments E1 and B2 and is probably representative of pore-free Alloy 10 fatigue life at 1300°F. For completeness the parabolic parameters which define this curve are presented in Table VII along with those for the three curves used to describe the 750°F fatigue data.

A meaningful comparison of Alloy 10 fatigue life at the two test temperatures can be made by examining the four parabolic curve fits and the 1300°F data points for heat treatment C2, Figure 15. At higher strain ranges the 1300°F fatigue life of Alloy 10 is similar to that of supersolvus Alloy 10 at 750°F, irrespective of heat treatment . As the

0.6% strain range is approached the 750 and 1300°F fatigue lives of subsolvus Alloy 10 begin to converge. Clearly comparison of 750 and 1300°F fatigue lives for supersolvus Alloy 10 is complicated by porosity issues at this strain range, and it would appear that porosity is limiting the 1300°F capability of Alloy 10. As HIP treatments are often used to reduce porosity, one could speculate that a HIP treatment might improve the fatigue life of supersolvus Alloy 10 at 1300°F, especially at lower strain ranges. This is clearly an area for future research.

Before summarizing the effects of heat treatment on Alloy 10 fatigue behavior it is worthwhile noting that one is studying mean life in this paper. Minimum life, which often limits disk designs, is affected by the "rogue" pore, scratch, or inclusion and requires much more data than that obtained in this report. As an example, a "realistic" minimum data point can be seen in Figure 13, note the B2 data point at .85% (approximately 1000 cycle life). Fractographic examination of the specimen revealed a surface inclusion at the initiation site, Figure 16. These issues are therefore as important as the heat treatment issues which are the subject of this paper.

SUMMARY AND CONCLUSIONS

As part of NASA's Ultrasafe Project the fatigue properties of Alloy 10, a high strength, nickel-base disk alloy, were evaluated for eight heat treat options. These heat treatments were designed to study the effects of solution temperature, cooling rate, and stabilization. At 750°F, a typical bore temperature for disk applications, solution temperature was found to have the greatest impact on fatigue life. Lower solution temperatures produced longer fatigue lives. The improvement in fatigue life at lower solution temperatures was most likely produced by finer grain sizes at this temperature. At 1300°F, a fairly aggressive rim temperature, the fatigue life of Alloy 10 was found to be relatively insensitive to heat treatment at high strains. At lower strains, such as 0.6%, fatigue life was again affected by solution temperature, with lower solution temperatures yielding longer fatigue lives. However, in this instance porosity, which increased as solution temperatures increased, appeared to limit fatigue life at 1300°F. Application of high pressures, i.e. HIP treatment, especially at higher solution temperatures may alleviate this problem.

REFERENCES

1. Jain, S. K., Regional Engine Disk Process Development Final Report, NASA Contract NAS3-27720 Task 4.2.4, September 1999.

Table I. Composition of Alloy 10 in weight percent.

Cr	Co	Al	Ti	Nb	Mo	W	Ta	C	B	Zr	Ni
10.2	14.9	3.69	3.93	1.87	2.73	6.2	0.9	.03	.03	.10	Bal

Table II. Heat treatment.

Serial Number	Solution (2.5Hours)	Cooling Rate	Stabilization	Code
B1	2125F	Fan	None	SUB/FAN
B2	2125F	Oil Quench	None	SUB/OIL
C1	2125F	Oil Quench	1550F/4HR	SUB/OIL/STAB
D2	2160F	1200F Molten Salt Bath	None	NEAR/SALT
E1	2160F	Fan	None	NEAR/FAN
D1	2190F	Fan	None	SUP/FAN
C2	2190F	Fan	1550F/4HR	SUP/FAN/STAB
E2	2190F	3F/MIN to 2160F then Fan	None	SUP/CONT

Table III. Grain size and cooling γ' size .

Serial Number	Code	Cooling γ' Size (μ m)	ASTM Gain Size
B1	SUB/FAN	0.3	11.3
B2	SUB/OIL	0.2	11.5
C1	SUB/OIL/STAB	0.2	11.5
D2	SUB/SALT	0.2	12.1
E1	NEAR/FAN	0.4	7.7
D1	SUP/FAN	0.4	6.1
C2	SUP/FAN/STAB	0.5	6.4
E2	SUP/CONT	0.5	6.4

Note: D2's actual solution temperature was probably closer to 2025°F as it has the finest grain size of all heat treatments. Its code has therefore been changed to SUB/SALT.

Table IV. Regression results for parabolic fit of stress range data.

Regression results for stress range at 750°F.

Code	Serial Number	A	B
SUB/FAN	B1	326.91	-52.00
SUB/OIL	B2	318.81	-38.71
SUB/OIL/STAB	C1	320.69	-35.21
SUB/SALT	D2	335.50	-58.16
NEAR/FAN	E1	324.64	-44.14
SUP/FAN	D1	333.04	-57.35
SUP/FAN/STAB	C2	338.67	-61.99
SUP/CONT	E2	336.03	-61.43

$STRESS_{RANGE}=A*STRAIN+B*STRAIN^2$

Regression results for stress range at 1300°F.

Code	Serial Number	A	B
SUB/OIL	B2	276.48	-34.35
NEAR/FAN	E1	287.98	-48.19
SUP/FAN/STAB	C2	281.29	-41.65

$STRESS_{RANGE}=A*STRAIN+B*STRAIN^2$

STRAIN = %

STRESS=KSI

Table V. Regression result for linear fit of maximum stress data.

Regression results for maximum stress at 750°F.

Code	Serial Number	A	B
SUB/FAN	B1	155.14	20.61
SUB/OIL	B2	155.47	27.28
SUB/OIL/STAB	C1	151.07	33.86
SUB/SALT	D2	155.43	19.58
NEAR/FAN	E1	134.10	38.20
SUP/FAN	D1	132.61	32.20
SUP/FAN/STAB	C2	135.47	30.11
SUP/CONT	E2	133.13	30.20

$STRESS_{MAX}=A+B*STRAIN$

Regression results for maximum stress at 1300°F.

Code	Serial Number	A	B
SUB/OIL	B2	137.75	30.20
NEAR/FAN	E1	131.41	23.23
SUP/FAN/STAB	C2	125.00	27.34

$STRESS_{MAX}=A+B*STRAIN$

STRAIN = %

STRESS=KSI

Table VI. Inelastic strain at half life for fatigue tests run at 1.4% total strain.

Code	Serial Number	Test Temperature(F)	Yield Strength(KSI)	Inelastic Strain(%)
SUB/FAN	B1	750	173	.12
SUB/OIL	B2	750	186	.08
SUB/OIL/STAB	C1	750	186	.08
SUB/SALT	D2	750	177	.12
NEAR/FAN	E1	750	169	.10
SUP/FAN	D1	750	164	.16
SUP/FAN/STAB	C2	750	163	.14
SUP/CONT	E2	750	161	.14
SUB/OIL	B2	1300	175	.15
NEAR/FAN	E1	1300	157	.21
SUP/FAN/STAB	C2	1300	153	.19

Table VII. Regression results for parabolic fit of fatigue life data.

Heat Treat	Temperature(F)	A	B	C
All Subsolvus	750	4.723	-1.2840	0.0979
E1	750	3.915	-0.9043	0.0478
All Supersolvus	750	3.808	-1.0555	0.0788
E1 & C2	1300	3.627	-1.1350	0.1060

$$\text{STRAIN RANGE} = A + B*\text{LOG}_{10}(N_f) + C*(\text{LOG}_{10}(N_f))^2$$

STRAIN RANGE = %

N_f = LIFE IN CYCLES

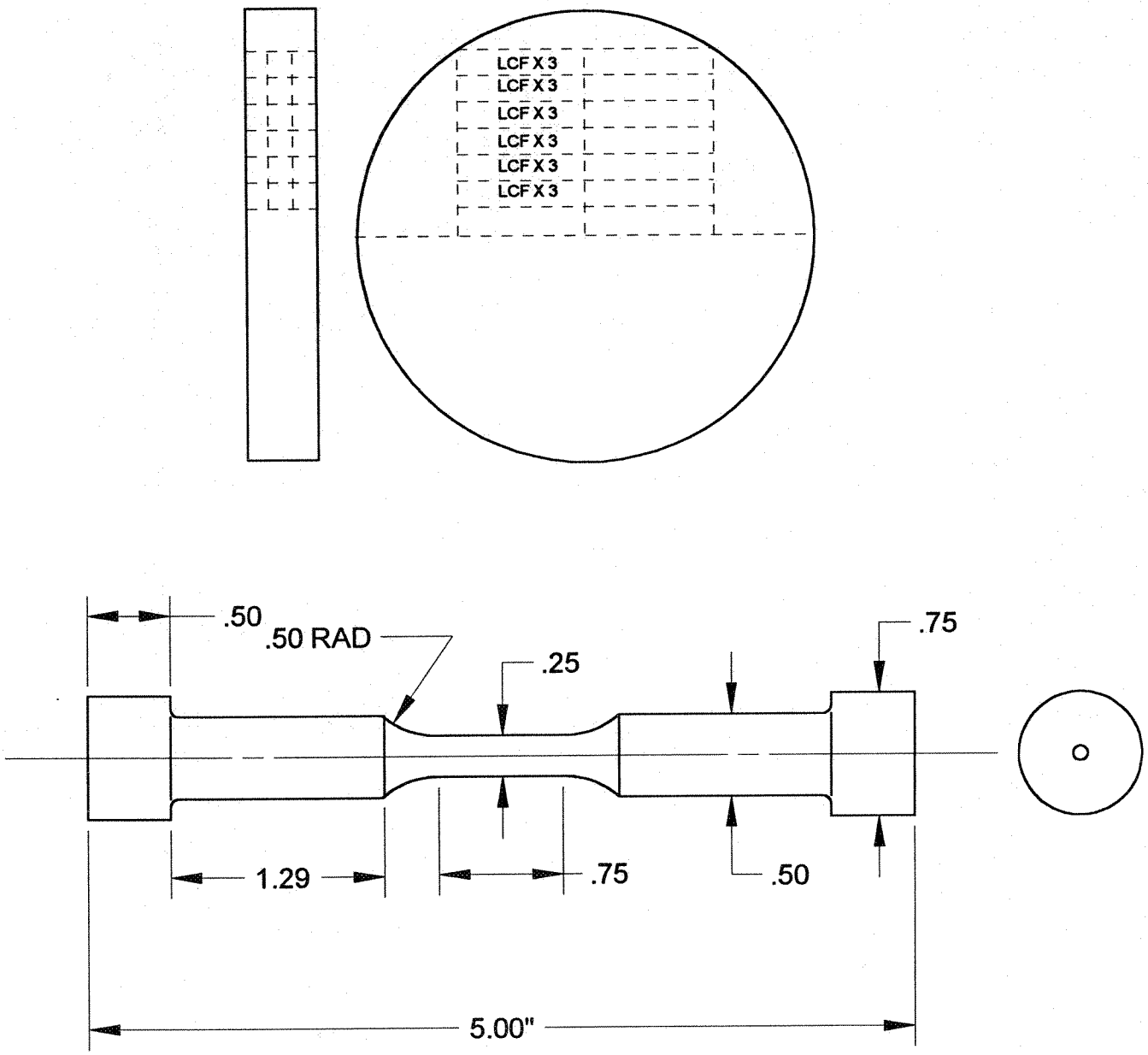

FIGURE 1. DESIGN OF FATIGUE SPECIMEN & CUT UP PLAN FOR FORGINGS.

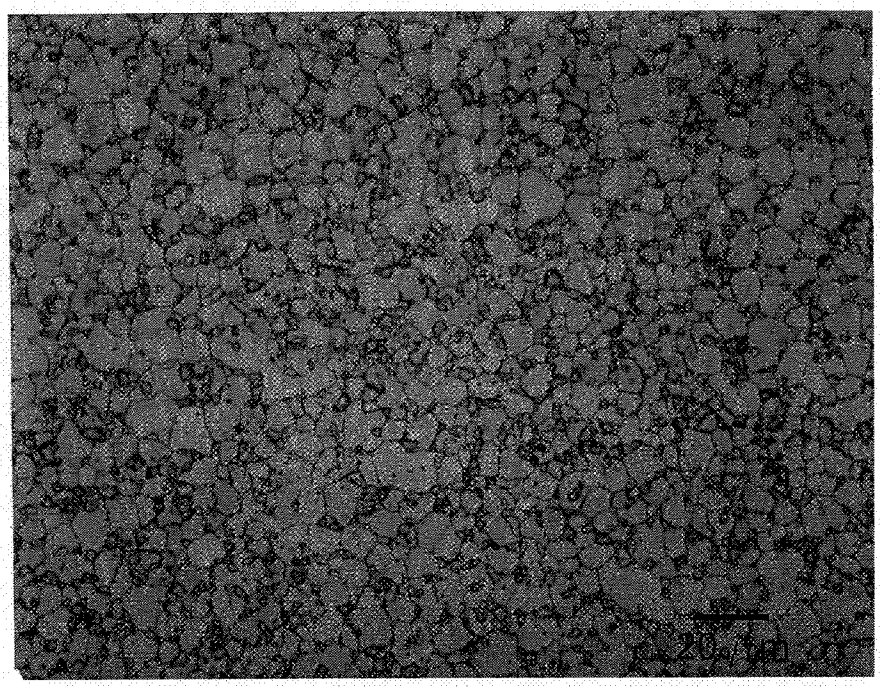

ESSENTIALLY PORE FREE SUBSOLVUS MICROSTRUCTURE

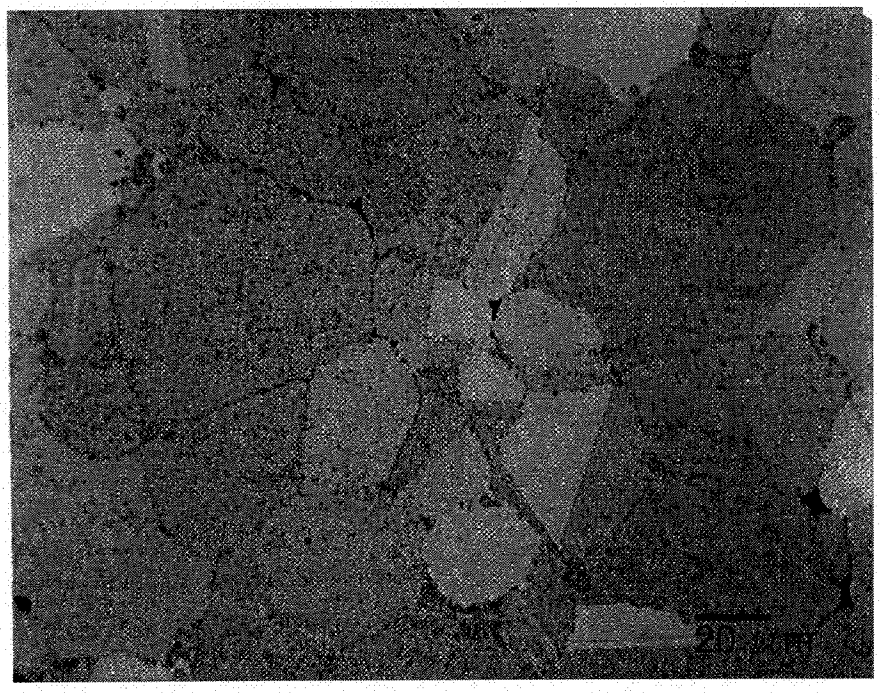

SUPERSOLVUS MICROSTRUCTURE WITH TRIPLE POINT POROSITY

FIGURE 2. POROSITY CONTENTS IN ALLOY 10

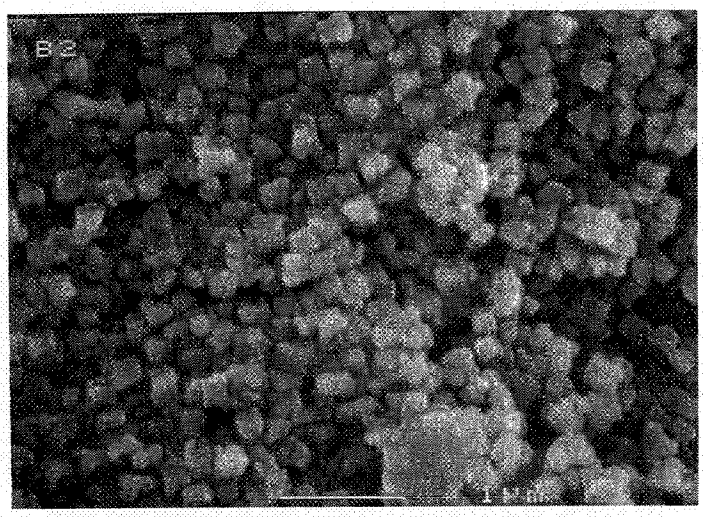

SUBSOLVUS/OIL QUENCHED

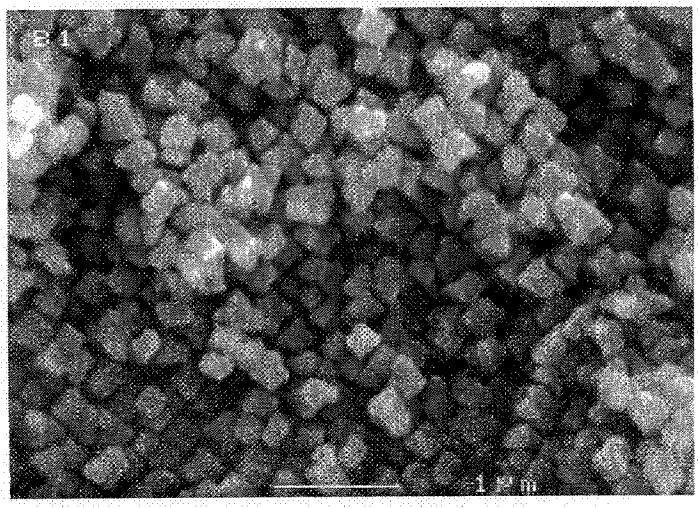

SUBSOLVUS/FAN COOLED

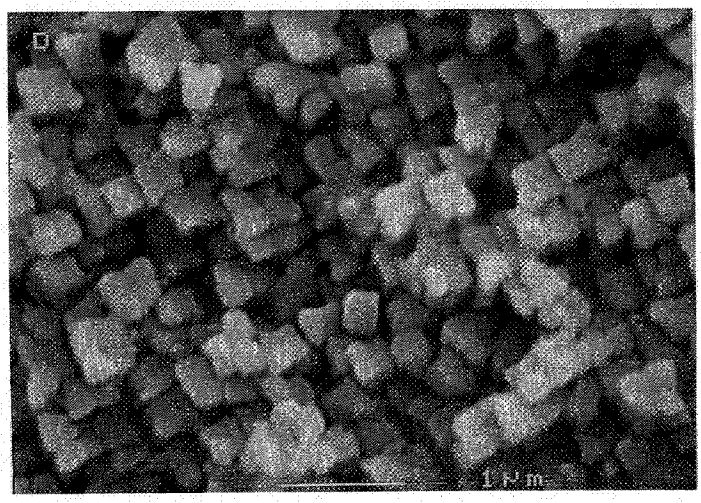

SUPERSOLVUS/FAN COOLED

FIGURE 3. COOLING GAMMA PRIME

FIGURE 4. ALLOY 10 TENSILE PROPERTIES AT 800F.

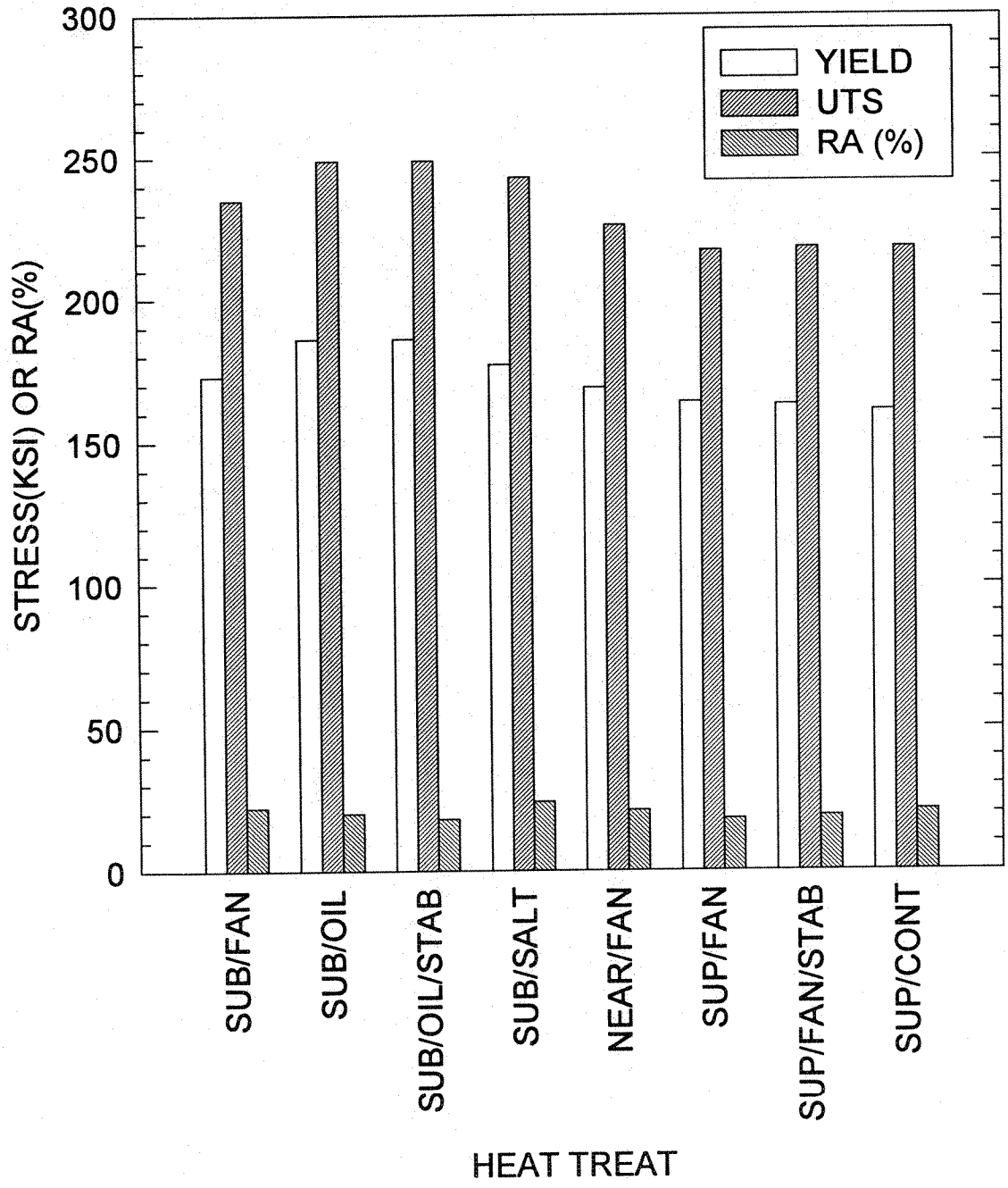

FIGURE 5. ALLOY 10 TENSILE PROPERTIES AT 1300F.

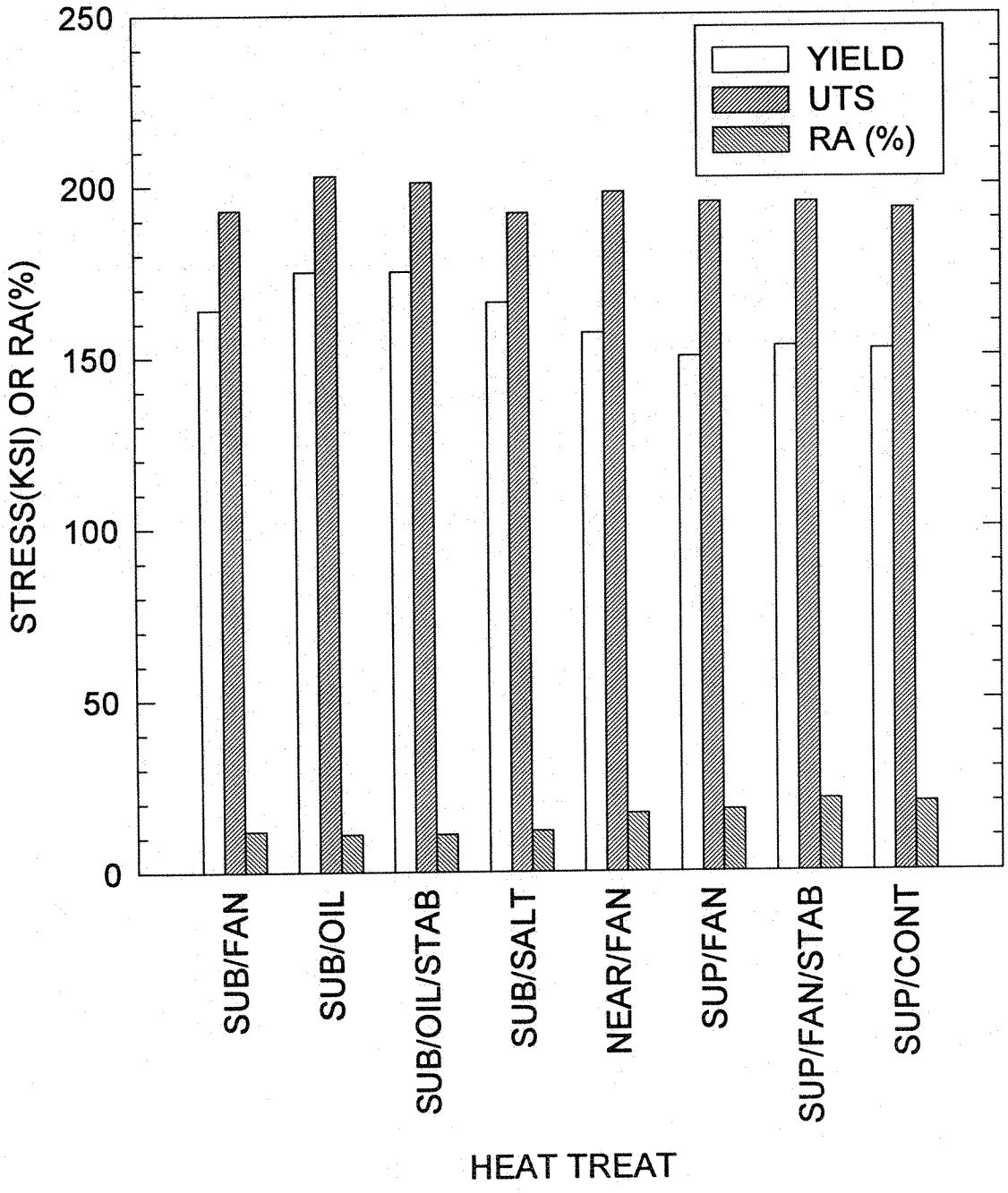

FIGURE 6. CREEP DATA AT 1300F/100KSI.

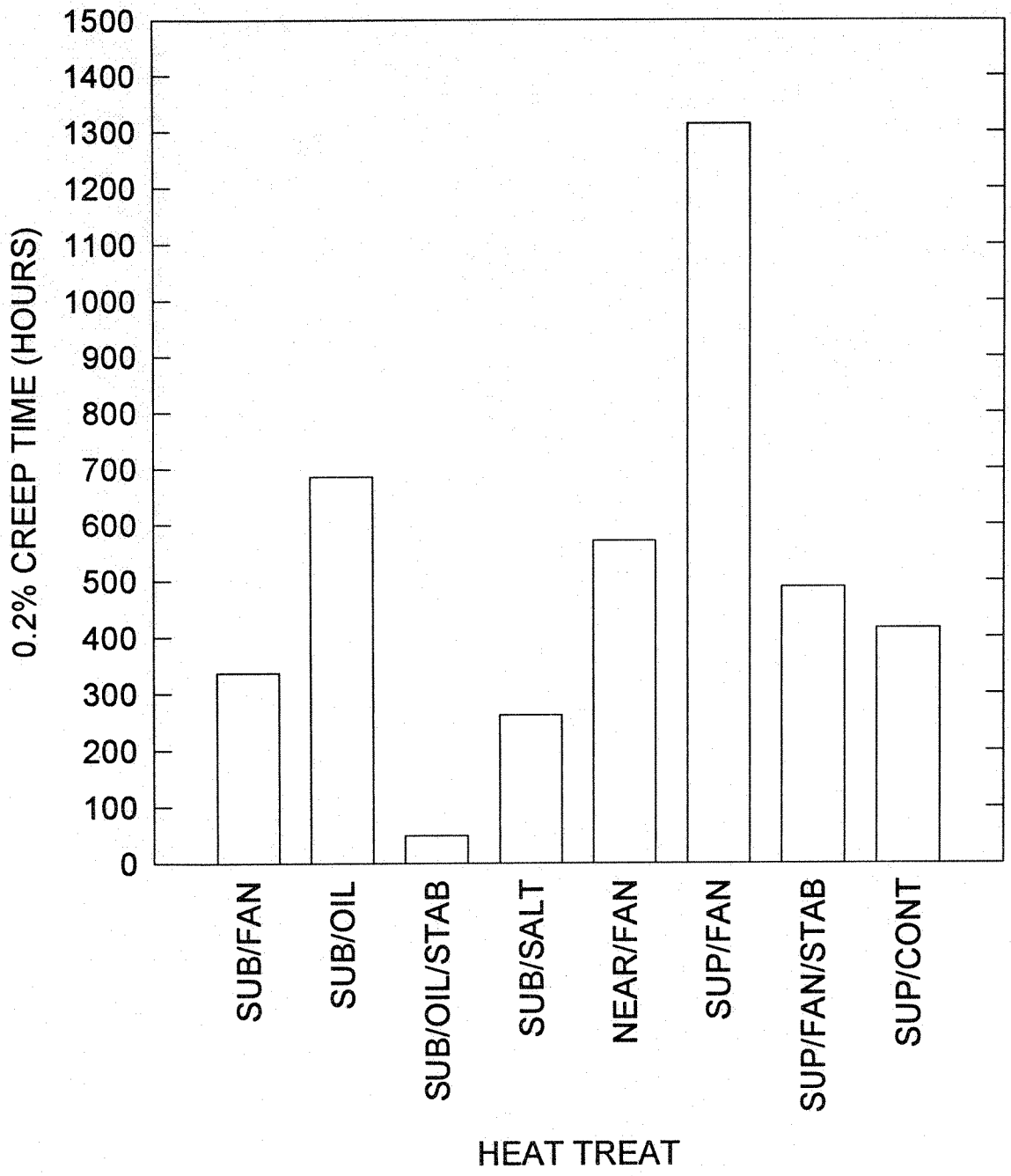

FIGURE 7. CYCLIC STRESS-STRAIN PLOTS.

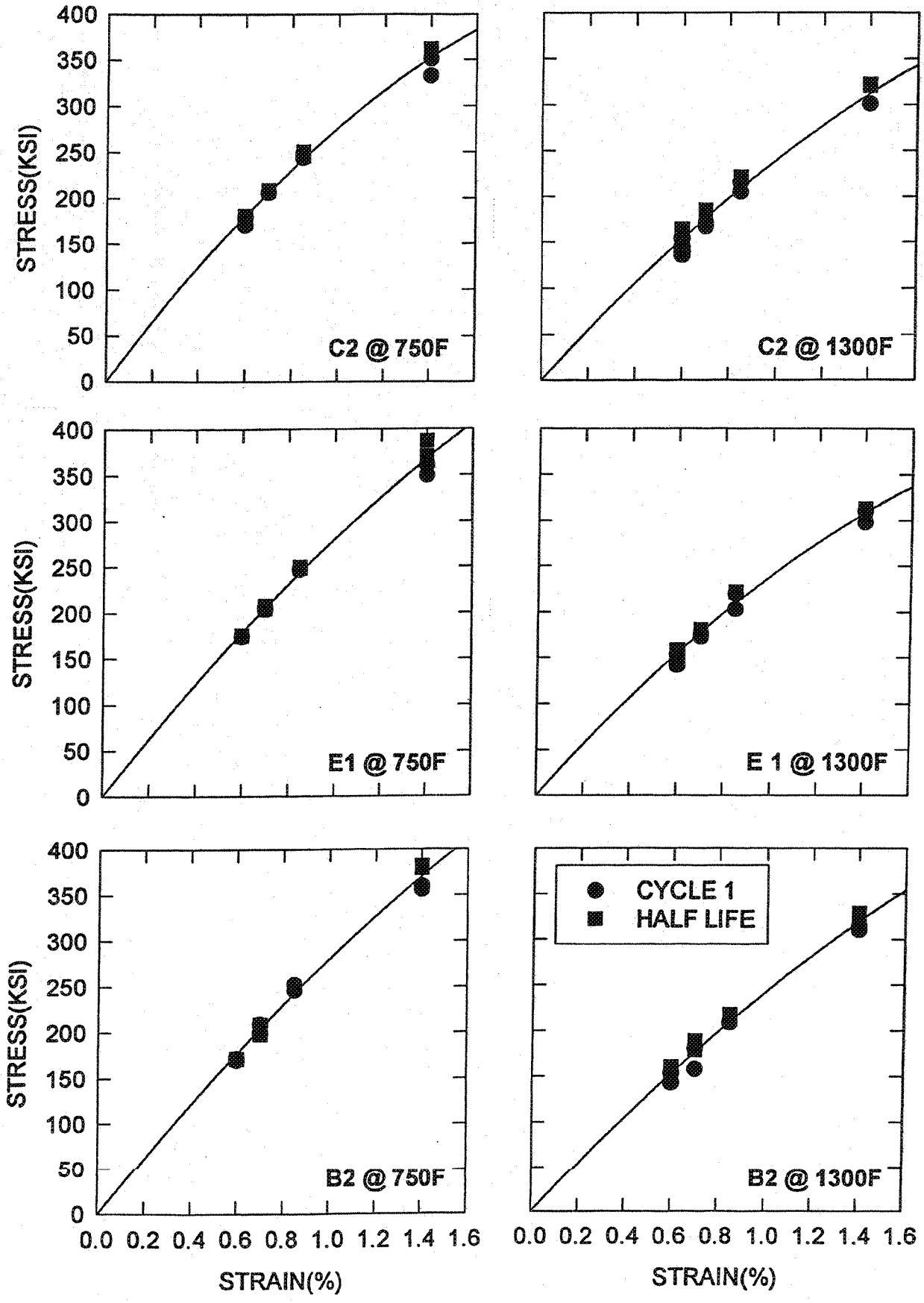

FIGURE 8. STRESS RANGE VERSUS YIELD STRENGTH.

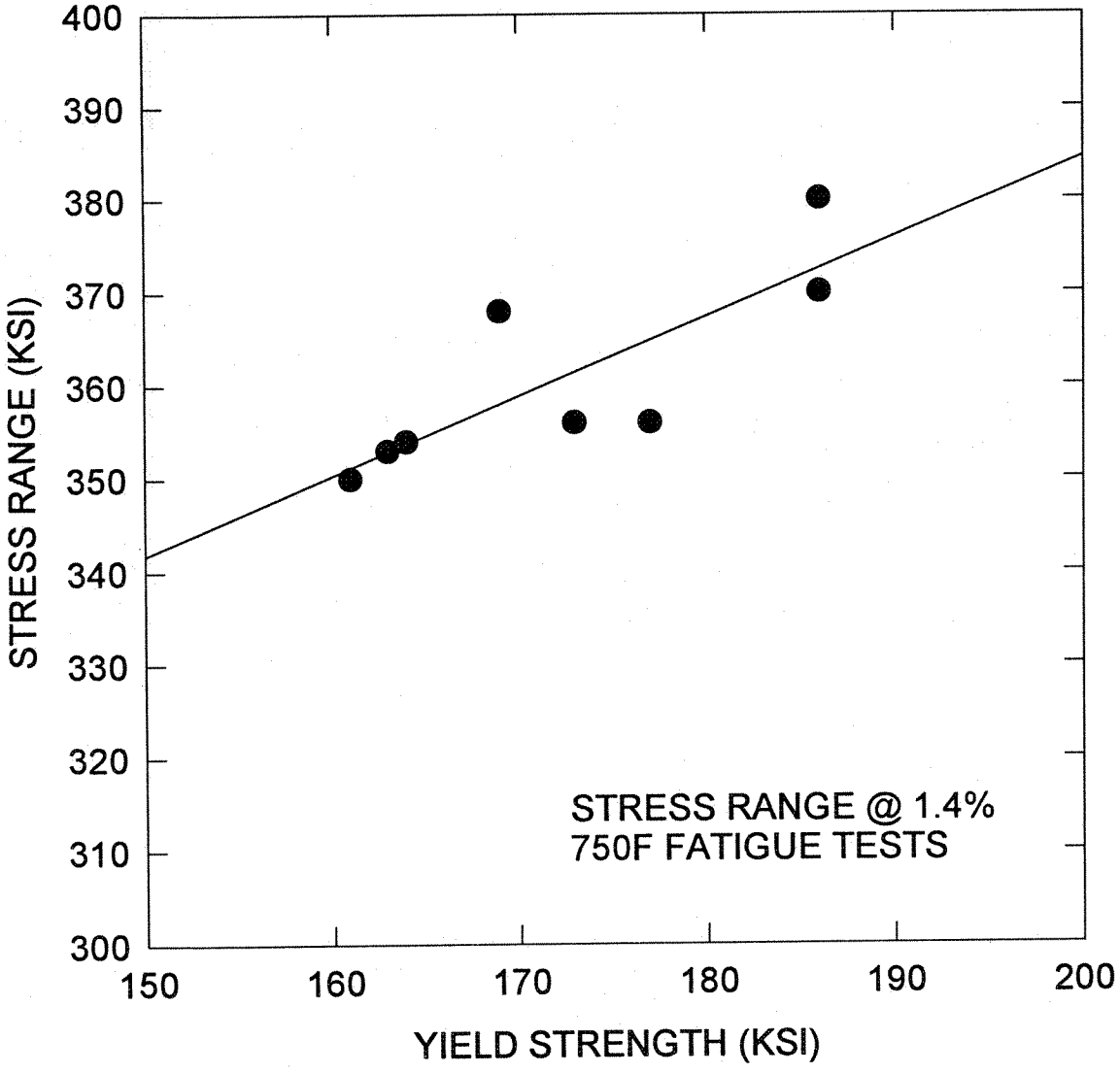

FIGURE 9. MAXIMUM STRESS PLOTS.

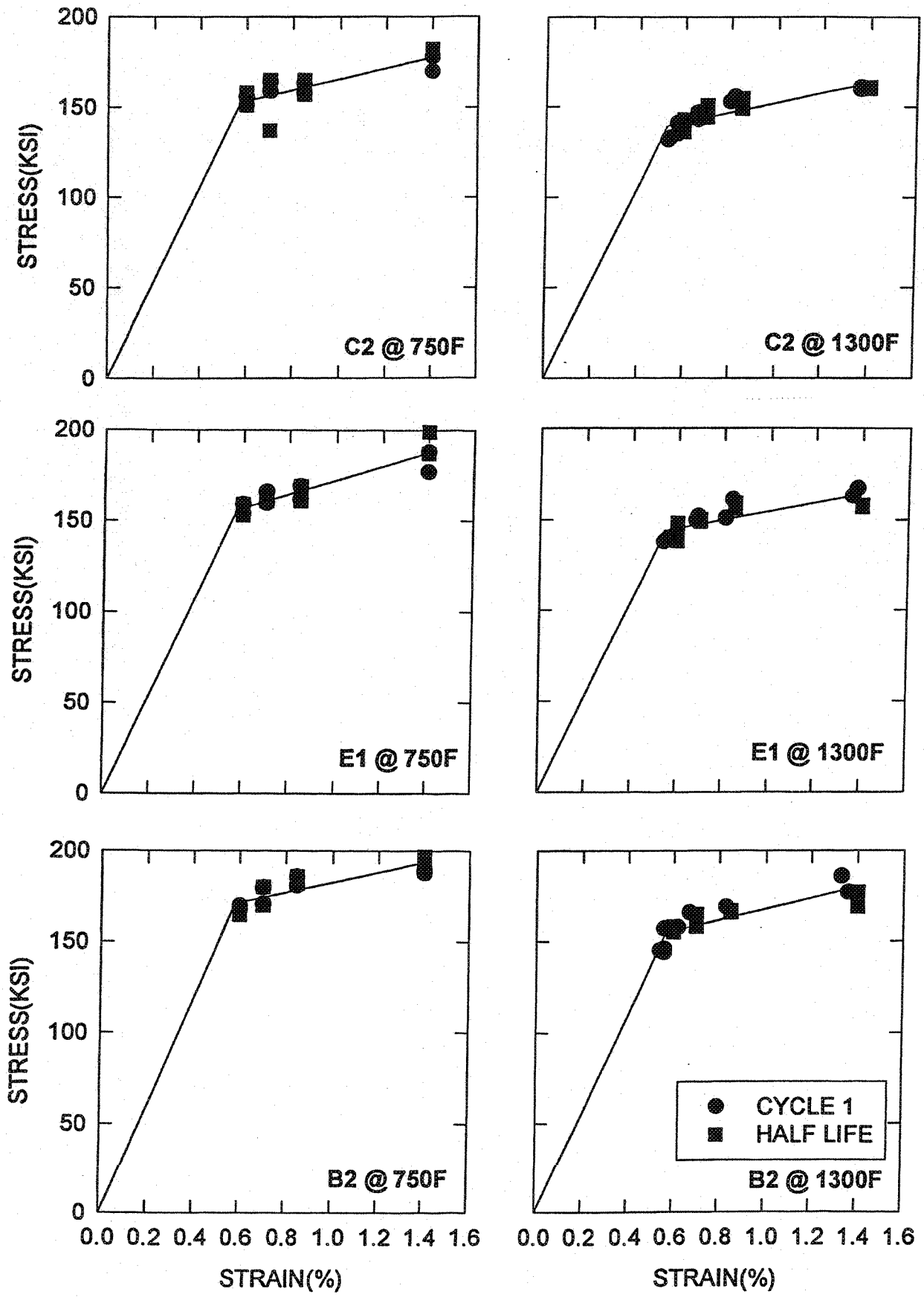

FIGURE 10. MAXIMUM STRESS VERSUS YIELD STRENGTH.

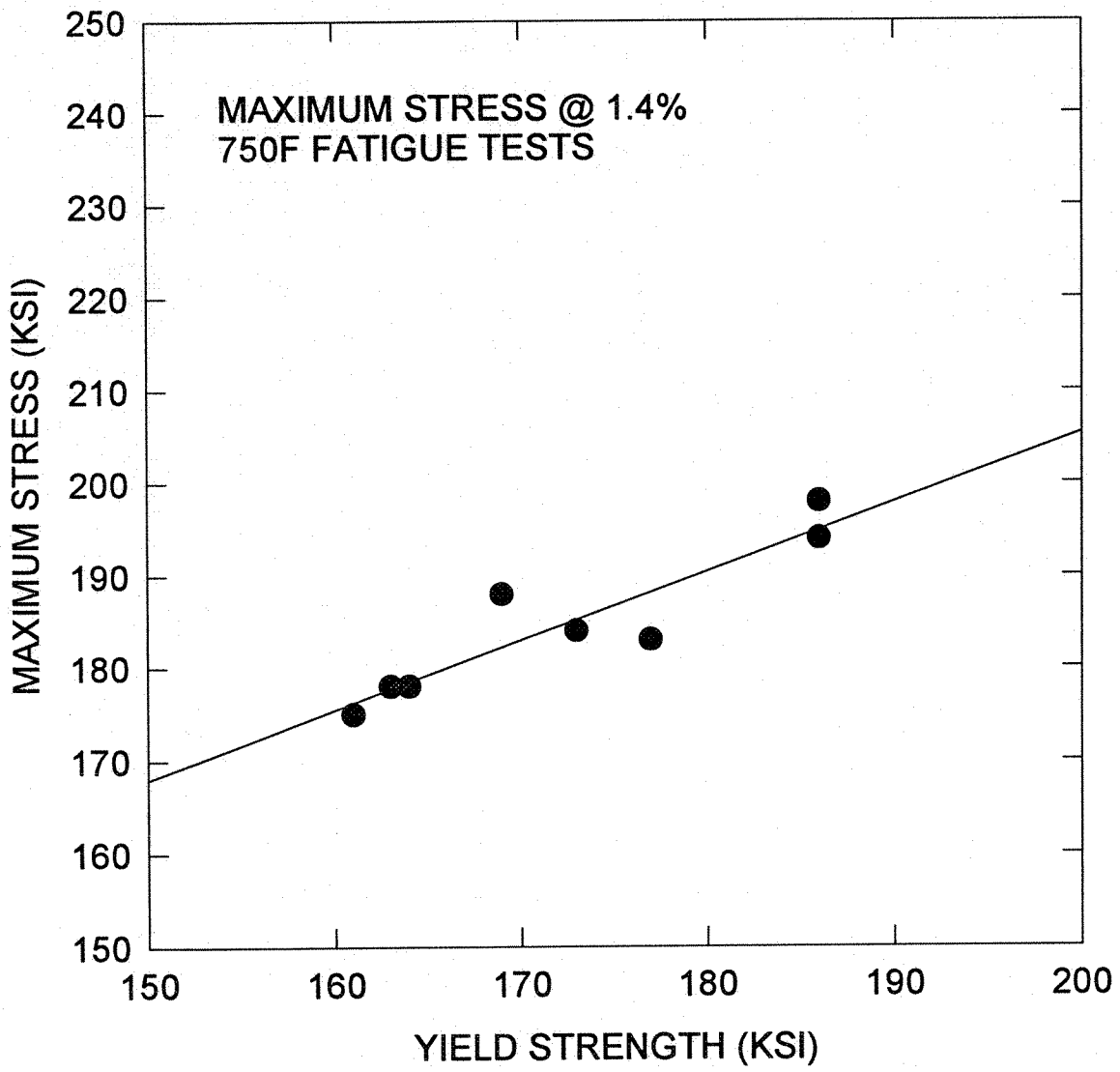

FIGURE 11. ALLOY 10 FATIGUE LIFE AT 750F.

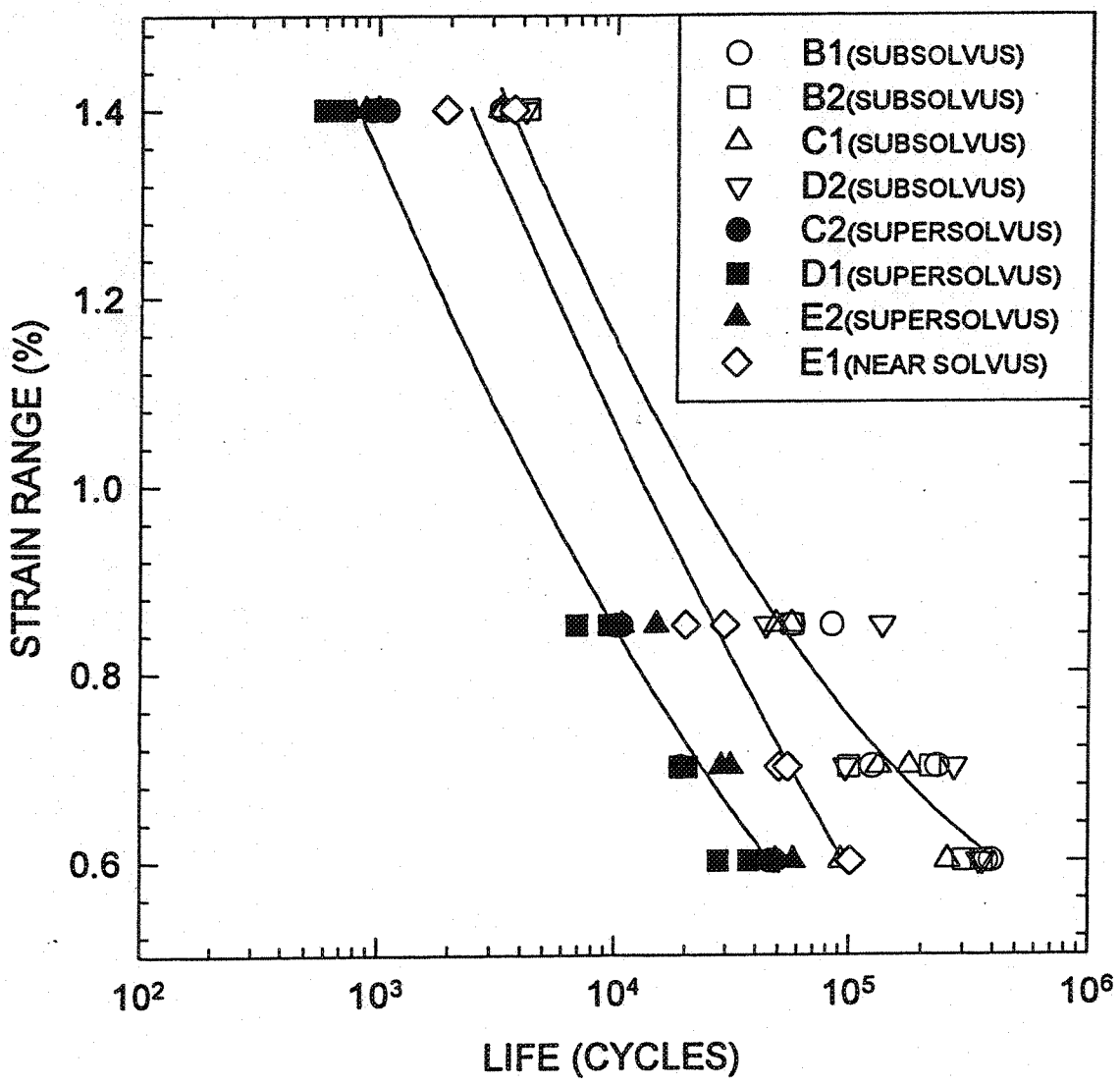

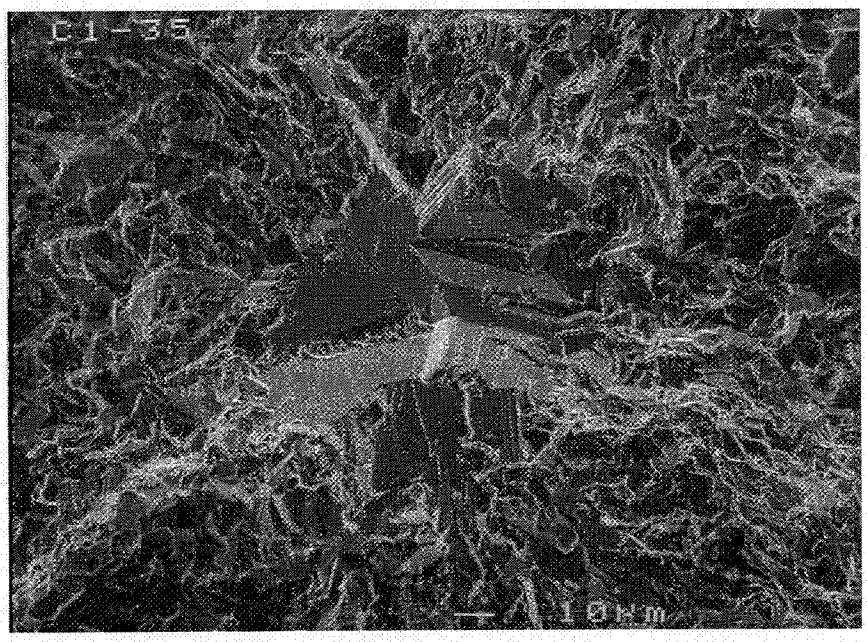

SUBSOLVUS

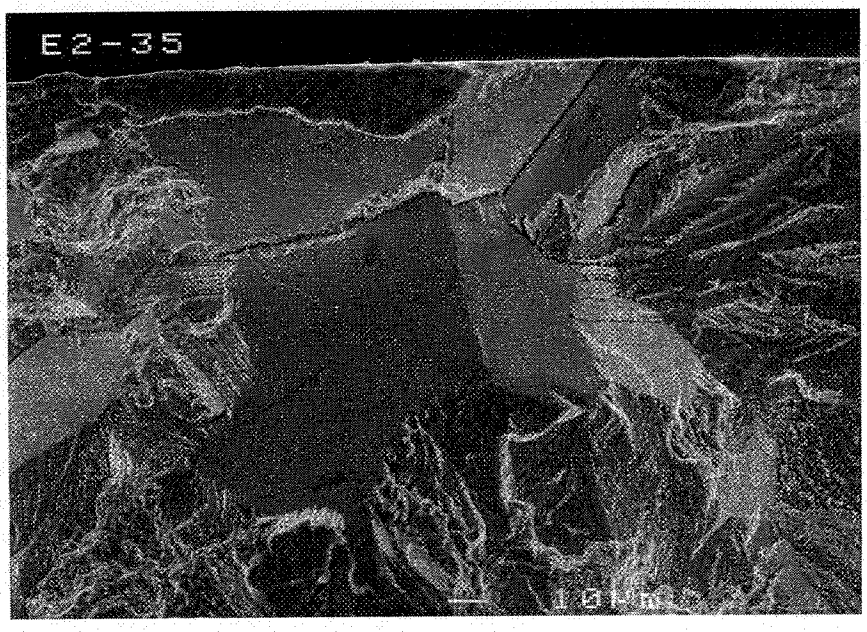

SUPERSOLVUS

FIGURE 12. FACET INITIATION PREDOMINANT AT 750°F

FIGURE 13. ALLOY 10 FATIGUE LIFE AT 1300F.

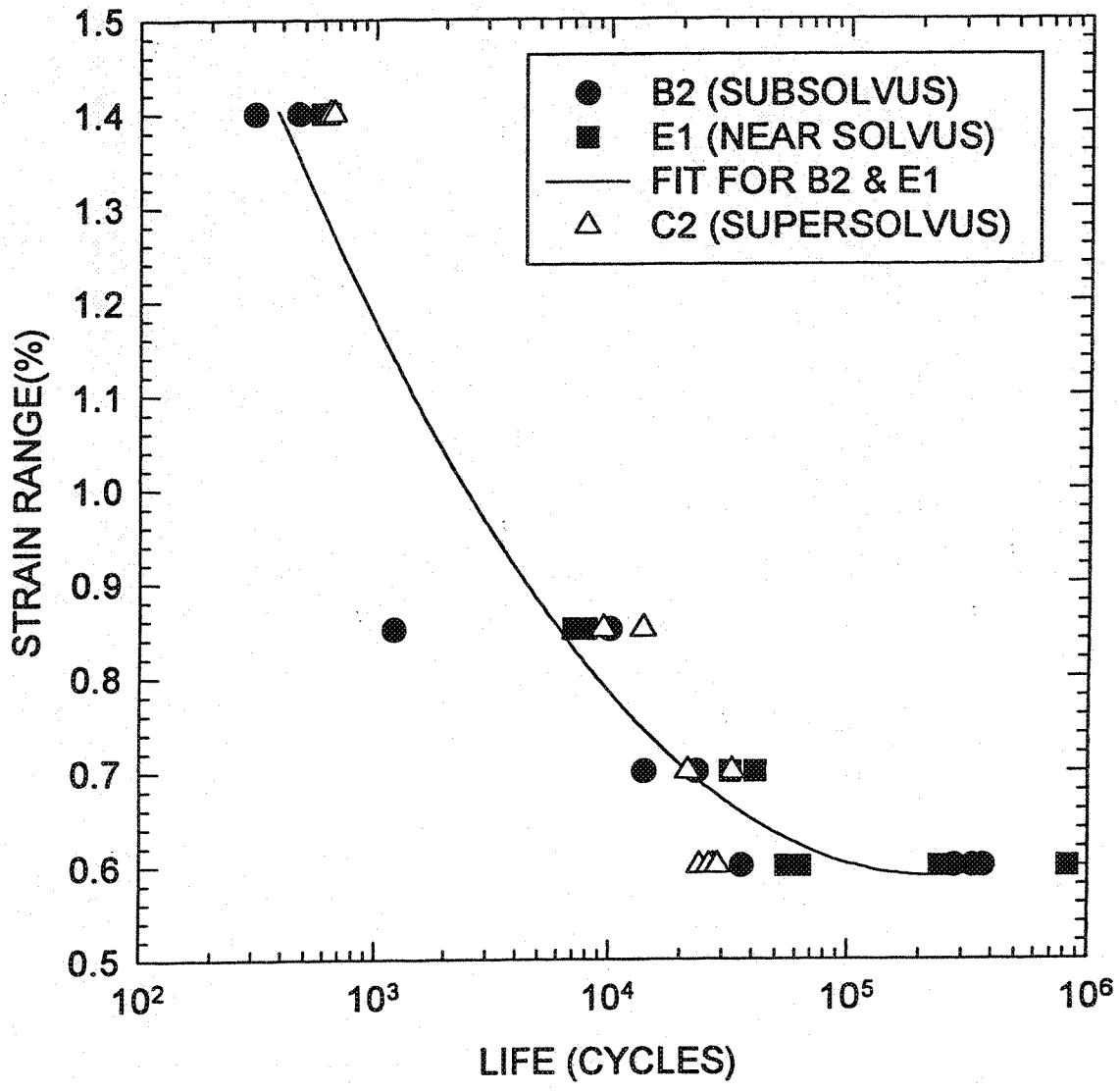

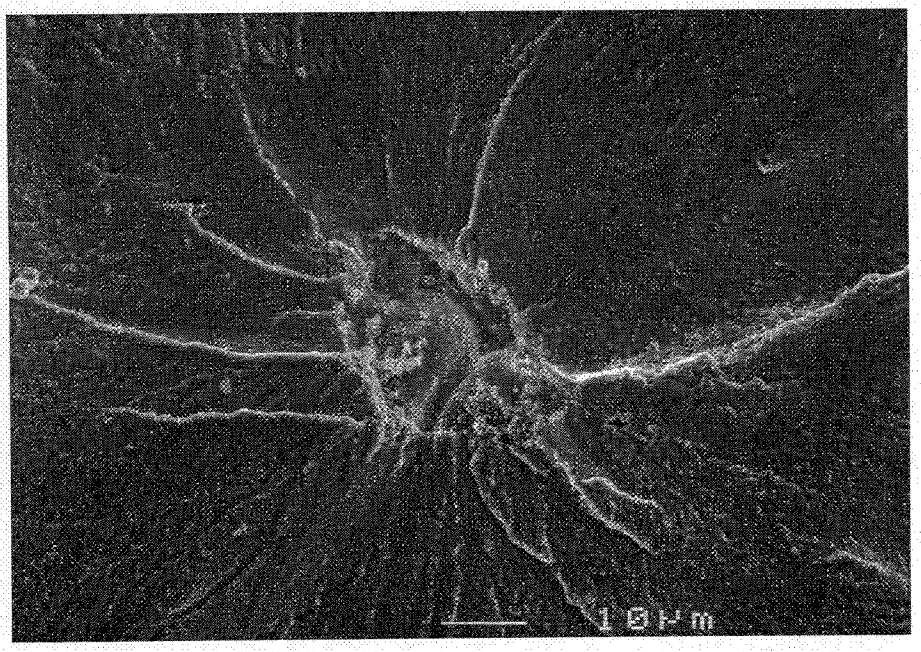

FIGURE 14. PORE RELATED FAILURE AT 1300°F

FIGURE 15. ALLOY 10 FATIGUE LIFE AT 750 AND 1300F.

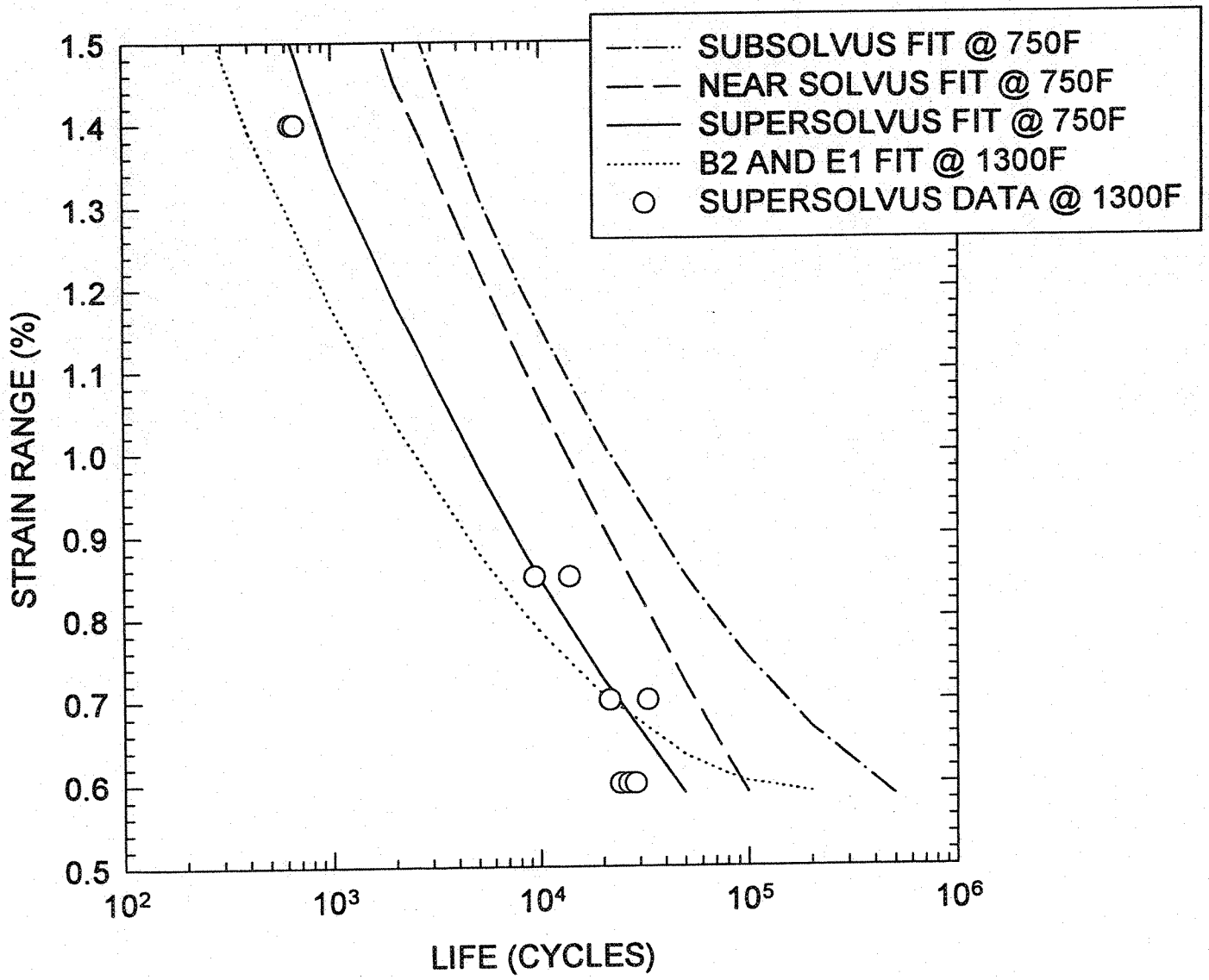

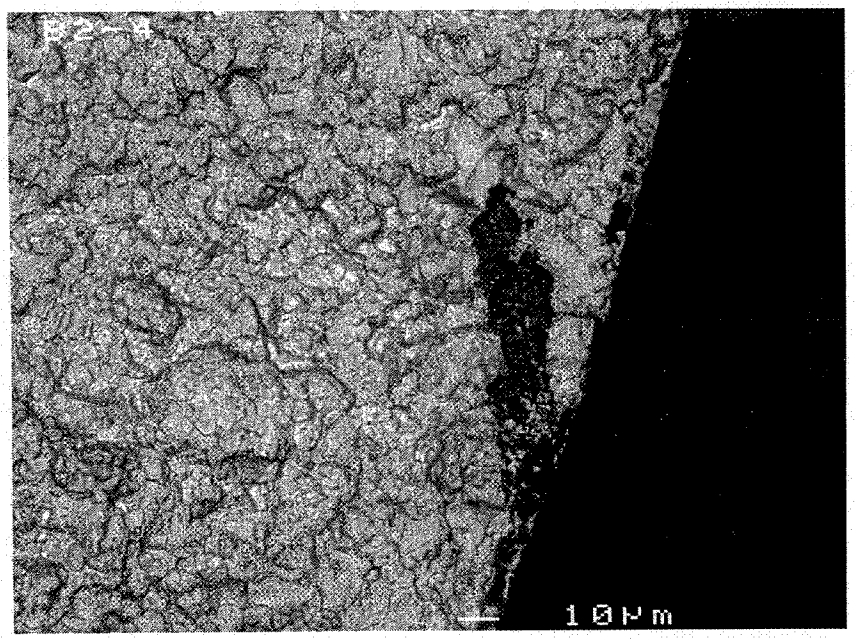

FIGURE 16. SURFACE INCLUSION IN SPECIMEN B2-4

REPORT DOCUMENTATION PAGE

Form Approved
OMB No. 0704-0188

1. AGENCY USE ONLY (*Leave blank*)	2. REPORT DATE	3. REPORT TYPE AND DATES COVERED
	August 2003	Technical Memorandum

4. TITLE AND SUBTITLE

The Effect of Heat Treatment on the Fatigue Behavior of Alloy 10

5. FUNDING NUMBERS

WU–708–24–13–00

6. AUTHOR(S)

John Gayda, Pete Kantzos, and Jack Telesman

7. PERFORMING ORGANIZATION NAME(S) AND ADDRESS(ES)

National Aeronautics and Space Administration
John H. Glenn Research Center at Lewis Field
Cleveland, Ohio 44135–3191

8. PERFORMING ORGANIZATION REPORT NUMBER

E–14011

9. SPONSORING/MONITORING AGENCY NAME(S) AND ADDRESS(ES)

National Aeronautics and Space Administration
Washington, DC 20546–0001

10. SPONSORING/MONITORING AGENCY REPORT NUMBER

NASA TM—2003-212473

11. SUPPLEMENTARY NOTES

This research was originally published internally as AST032 in February 2000. John Gayda and Jack Telesman, NASA Glenn Research Center; and Pete Kantzos, Ohio Aerospace Institute, Brook Park, Ohio 44142. Responsible person, John Gayda, organization code 5120, 216–433–3273.

12a. DISTRIBUTION/AVAILABILITY STATEMENT

Unclassified - Unlimited
Subject Category: 26 Distribution: Nonstandard

Available electronically at http://gltrs.grc.nasa.gov

This publication is available from the NASA Center for AeroSpace Information, 301–621–0390.

12b. DISTRIBUTION CODE

13. ABSTRACT ***(Maximum 200 words)***

The results of the fatigue evaluation on Alloy 10, run under NASA's Ultrasafe Project, are the subject of this report. Crack growth evaluation will be examined in a separate report. The eight heat treatments studied were designed to evaluate the effect of solution temperature, cooling rate, and stabilization on key mechanical properties of Alloy 10, including fatigue life. Two temperatures were studied, 750 and 1300 °F, which represent projected application temperatures for the bore and rim locations in a disk. In addition to fatigue life, the cyclic stress-strain response and failure modes of the fatigue specimens are also reviewed in this report.

14. SUBJECT TERMS

Superalloys; Disk

15. NUMBER OF PAGES

30

16. PRICE CODE

17. SECURITY CLASSIFICATION OF REPORT	18. SECURITY CLASSIFICATION OF THIS PAGE	19. SECURITY CLASSIFICATION OF ABSTRACT	20. LIMITATION OF ABSTRACT
Unclassified	Unclassified	Unclassified	